M. L. Tanaka

Influence of Storage Environment Upon Crack Opening and Growth in a Particulate Composite

C.W. Smith[a], L. Wang[b], and M.L. Tanaka[c]
Department of Engineering Science and Mechanics
Virginia Polytechnic Institute and State University
Blacksburg, Virginia 24061

ABSTRACT

Defects formed in solid rocket propellant during manufacturing, transportation, storage, and assembly can lead to alterations in the thrust time profiles and possibly catastrophic failure of the entire rocket. In order to determine the effects of temperature, loading rate, and thickness on this particulate composite, tests were conducted at three temperatures, two loading rates, and two thicknesses. Both uncracked and edge cracked "biaxial" specimens were produced from solid rocket propellant. The stress relaxation modulus and stress strain data were obtained from load curves formed during "biaxial" tension tests. Near crack tip displacements and strains were calculated from photographs taken of a surface grating on the pre-cracked specimens during crack propagation. The effect of thickness on the stress intensity factor at crack initiation and maximum stress intensity factor also were studied. Finally, by applying continuum theory the displacement singularity was determined at different stages of crack growth.

From the stress strain data, it was found that the effect of temperature had a greater influence on the behavior than did loading rate for the temperatures and loading rates studied. The crack growth in the composite consists of a series of crack opening, crack blunting, and crack growth/resharpening stages which are highly nonlinear. A single stress intensity factor was determined at crack initiation and found to be independent of thickness. However, during crack growth the maximum SIF was found to be lower in the thick specimens due to more and larger voids. Determination of the displacement singularity order for the sharp cracks was found to be consistent with the theoretical results predicted by Benthem.

INTRODUCTION

Solid rocket propellant is a particulate composite consisting of powdered aluminum and ammonium salt bound by a polymeric matrix. Propellant not only serves as fuel but also as a structural component for the entire rocket. Defects and cracks formed during manufacturing, transportation, storage and assembly have been found which alter the thrust-time profile and can lead to catastrophic failure of the entire structure. By studying the material's failure mechanism under varying conditions, safety and control may be improved.

The senior author and his colleagues have conducted extensive work on inert propellant to determine its failure mechanism [1, 2, 3]. The current research examines the effects of thickness, loading rate, and temperature on real propellant with ranges simulating actual storage conditions.

Motor grain material, due to its lack of stiffness particularly at room and elevated temperature, presents some special problems when loaded mechanically. Gripping must be done by gluing and the measurement of near tip surface displacements must be accomplished by a measuring system which does not affect the material stiffness. Moreover, measurements must not be too fine if continuum type algorithms are to be employed. Finally , "biaxial" specimens are normally employed to induce some transverse constraint which is always present in the motor grain in service.

---

a: Alumni Professor
b: Research Associate
c: Graduate Research Assistant

TEST SPECIMENS AND PROCEDURES

Specimens of real propellant were received from the manufacturer as a 2"x8"x0.5" sheet (51mm x 203mm x 12.7mm). These specimens were cut to simulate the biaxial stress condition that often occurs during the propellant's lifetime (fig.1). The circular grooves cut from both sides were designed to prevent premature failure near the bonded area. Specimens were bonded to aluminum grips (fig.1) with epoxy [Hardman - Red 04001] and allowed to cure for at least 24 hours. These specimens were then tested to determine the stress-strain characteristics and stress relaxation data. In order to determine the crack growth and propagation characteristics, the following specimen was produced.

Pre-cracked specimens were formed by cutting a circular groove on one side. A 25.4mm crack was cut in the other side (fig.2) and a 5 line/mm grating was applied to the specimen at the crack tip region. Although finer gratings are available, the 0.2mm grating was chosen since its size corresponds to about half of that of the largest particle, 0.5mm. The use of this size grating partially masks the local particle effects and allows continuum theory to be applied. The foundation for the grating consists of a white paste produced by mixing titanium oxide and silicon grease. A thin layer was applied to the specimen around the crack tip and a metal screen of 5 lines/mm was carefully laid over the paste. The specimen was placed into a vacuum chamber where a piece of aluminum was evaporated and allowed to condense onto the surface. The aluminum reacted with the paste not covered by the screen turning it black. This resulted in a pattern of white lines on a black background when the screen was removed. The specimens were then fixed to the grips in the same manner as before.

Tests were conducted on both cracked and uncracked specimens at two loading rates, 2.54 and 12.7 mm/min., and three temperatures, -65, 72, 165 °F (-54, 22, 74 °C). On the uncracked specimen, tensile tests were conducted at constant head rates while stress relaxation tests involved an almost instantaneous loading to 3% global strain after which displacement was held constant. For the cracked specimen a constant loading rate tensile test was also conducted. However, a camera with a zoom lens was positioned to photograph the near crack tip region every 10 seconds or 2 seconds for a low or high loading rate respectively (fig.3). From these photographs displacements and strains were calculated.

METHOD OF ANALYSIS AND RESULTS

After a viscoelastic material is strained to a given value, the stress developed in the material will slowly decrease with time. This is called stress relaxation and may be governed by the general equation

$$E_r(t) = E_0 + E_1 t^{-n}$$

Over the temperature range studied E_0 and n remain constant with values of 0.98N/mm^2 and 0.32 respectively. However, E_1 changes with temperature having values of 220, 7.73, and 2.14 for temperatures -65, 72, 165 °F respectively. The modulus verses time plot is shown in figure(4). By applying the time-temperature superposition principle to the elevated and room temperature data, a master curve was developed for room temperature material (fig.5). Figure 5 reveals that the temperature range examined lies within the transition between glassy and rubbery behavior.

By observing the photographs of cracked specimens, a pattern of crack opening, blunting and resharpening occurs which is qualitatively independent of temperature and loading rate (fig.6). To analyze the photographs, a digitizing board was employed to locate and store the grid intersection points. The points were then compared to the undeformed grid to calculate displacements and strains. Typical results are shown in figure 7. The regularity of the displacement field (fig 7a) suggests that this material may be described by continuum theory. Figure 7b reveals an intense strain zone ($e_2 > 0.15$) around the crack tip, the size of which increases with global strain. Near the crack surface away from the crack tip, nearly rigid body displacements are observed (fig.7a). In the intense strain zone around the crack tip the material exhibits profuse dewetting. As the crack propagates, the fracture surface undulates through the matrix avoiding large crystals. This conclusion was formed by observing the crack's meandering pattern in figure 8, and from the protruding crystals seen in the SEM picture (fig.9). The material's stress-strain response was also observed.

Load verses global extension for thin specimens is shown in figure 10. Examining three different temperatures and two different loading rates the low temperature tests exhibit an increase in strength of around five times that of room temperature. Elevated temperature showed only a modest decrease in strength of about 30%. Although increasing load rate tends to increase the maximum load, the effect is small in comparison to that of decreasing temperature. Since low temperature data is not yet available for the thick specimen, the thickness effect is only examined for room and elevated temperatures.

Figures (11&12) show the results of several tests with differing thicknesses, loading rates, and temperatures. By observing the graphs, it is seen that the maximum load per unit thickness decreases with increasing thickness. This phenomenon corresponds to a decreasing maximum stress intensity factor. Such an effect is well-known in metals and is due to transverse constraints in thicker specimens. However in rocket propellant, a particulate composite in a polymeric binder, the effect is conjectured to be due to voids. Griffith [4, 5] observed a similar effect in glass fibers. Based on molecular bond strengths, Griffith found a discrepancy between the theoretical strength of glass and the observed strength of the glass fibers. Griffith proceeded to conduct tests on specimens of ever decreasing diameter and discovered as specimen thickness decreased, strength increased. He attributed this occurrence to the presence of defects and concluded that as

thickness increased so did the possibility of a large defect, thus reducing its strength. In rocket propellant the defects are voids caused by dewetting of the crystals from the matrix. The point at which initial crack growth occurred is shown in table 1 and figures 11 and 12.

Table 1

	Thin		Thick	
	Time	Global Ext.	Time	Global Ext.
HR-RT	11 sec.	2.3 mm	12 sec.	2.5 mm
LR-RT	55 sec.	2.3 mm	75 sec.	3.2 mm
HR-ET	21 sec.	4.4 mm	19 sec.	4.0 mm
LR-ET	95 sec.	4.0 mm	85 sec.	3.6 mm

HR => High Rate 12.7 mm/min RT => Room Temperature 72 °F
LR => Low Rate 12.7 mm/min ET => Elevated Temperature 165 °F

The global extension at crack initiation is seen to increase with increasing temperature, yet remain relatively independent of loading rate and thickness. This implies that a single stress intensity factor exists at crack initiation that is independent of thickness. As the crack begins to propagate, the values of the stress intensity factor for the thick and thin specimen diverge from the initiation value. At this point the SIF for the thick specimen falls below that of the thin specimen as noted above.

It is well known that the stress singularity for a crack in the interior of a body is $r^{-1/2}$. This result corresponds to stress and displacement eigenvalues of $\lambda_s = -0.5$ and $\lambda_d = 0.5$, respectively. Benthem [6] predicted that when a crack intersected a free surface the dominant displacement eigenvalue would be increased to $\lambda_d = 0.67$ for an incompressible material. Although this result assumes an isotropic media, it may also apply to rocket propellant since the specimen is globally isotropic and only locally anisotropic. To determine the dominant displacement eigenvalue, lines normal to the crack plane were drawn on the photographs and the grid intersection points were digitized. Displacement eigenvalues shown in table 2 were calculated from a log-log plot using algorithms based upon Benthem's analysis (see appendix).

Table 2 Dominant Displacement Eigenvalue λ_d for Sharp Crack Tips

Temperature (F)	Loading Rate (mm/min.)	Thin (2.54mm) λ_d	Thick (12.7mm) λ_d
-65	12.7	0.70	-----
-65	2.54	0.67	-----
72	12.7	0.66	0.65
72	2.54	0.71	0.66
165	12.7	0.74	0.74
165	2.54	0.71	0.77

The average value of $\lambda_d = 0.70$ for the sharp crack agrees well with the theoretical value suggesting that continuum theory may apply. The result for the blunt crack (table 3) in the thin specimen was a higher value of 0.85. However, a different method is being used to determine the eigenvalues for the thick specimens. The previous method consisted of subtracting half of the crack tip opening displacement from the actual vertical displacements (see appendix). This method seemed to work well for the thin specimens but failed to give consistent results in the thick specimens. The new method yields more consistent results for the surface blunted crack by estimating the location of the sharp crack tip beneath the surface.

Table 3 Dominant Displacement Eigenvalue λ_d for Blunt Crack Tips

Temperature (F)	Loading Rate (mm/min.)	Thin (2.54mm) λ_d	Thick (12.7mm) λ_d
-65	12.7	0.82	-----
-65	2.54	0.88	-----
72	12.7	0.85	0.64
72	2.54	0.92	0.72
165	12.7	0.84	-----
165	2.54	0.84	-----

CONCLUSIONS

Tests conducted on real cracked rocket propellant show the materials to becomes stronger and less ductile with decreasing temperature. Relaxation tests determined that the temperature range studied fell within the glassy-rubbery transition. Increasing loading rate over the range studied had little effect on the results. The material has a single stress intensity factor at crack initiation which is independent of thickness. However, as the crack propagates the SIF is observed to decreases with increasing thickness. The good agreement between Benthem's theoretical and experimental displacement singularity implies that the material may be considered a continuum.

ACKNOWLEDGMENT

The authors wish to thank Mr. H. Mouille for his assistance, the suggestions of Dr. C.T. Liu, and the support of Phillips Laboratory AFSC under contract no. FO-4611-82-R-0011.

REFERENCES

1. Smith, C.W., Czarnek, R., and Rezvani, M., "Determination of Continuum Fracture Parameters for a Particulate Composite, " *J . of Engr. Materials and Technology,* ASME Trans., Vol. 112, No. 2, pp. 247-251, April, 1990.
2. Smith, C.W., Chang C.W., and Liu, C.T., "Measurement of Crack Induced Damage in Particulate Composites," *Proceedings of the 1990 SEM Spring Conference on Experimental Mechanics,* pp. 241-246, June 1990.
3. Smith, C.W. and Liu, C.T., "Effects of Near-Tip Behavior of Particulate Composites on Classical Concepts," *Composites Engineering An International J.*, Vol. 1, No.4 ,pp. 249-256, 1991
4. Griffith, A.A., "The Phenomena of Rupture and Flow in Solids," *Phil. Trans. R. Soc. London,* A221:163-198 (1921)
5. Griffith, A.A, "The Theory of Rupture," *Proc. 1st Int. Cong. Appl. Mech.,* Delft, 1925.
6. Benthem, J.P.,"The Quarter Infinite Crack in a Half Space; Alternative and Additional Solutions," *Int. J. of Solid and Structures*, Vol. 16, pp. 119-130.

APPENDIX

Algorithm for Displacement Singularity Determination

Benthem (6) studied the problem where a quarter infinite crack in a half space (figure A.1) intersects with the free surface at right angles. Benthem used the separation of variables method to evaluate the vertex singularity at the intersection point. He assumed

$$u_i = \sum_{k=1}^{\infty} r^{\lambda_u^k} h_i(\theta,\phi)_k \qquad (A.1)$$

By considering the vertical displacement along a line normal to the crack plane, a first order of approximation can be made.

$$u_2 = D_2 r^{\lambda_u} \qquad (A.2)$$

This leads to

$$\ln u_2 = \ln D_2 + \lambda_u \ln r \qquad (A.3)$$

The above equation can be utilized to estimate the displacement singularity, λ_u, for sharp crack tips by plotting $\ln(u_2)$ versus $\ln(r)$. For the blunted crack, the previous method modified equation (A.3) by subtracting half of the crack tip opening displacement, u_{20}, from the actual vertical displacement, u_2,

$$\ln(u_2-u_{20}) = \ln D_2 + \lambda_u \ln r \qquad (A.4)$$

While the method was adequate for the thin specimens, no consistent results were achieved for thick specimens. Thus, for the surface blunted crack, a new method was developed which estimates the location where the tip of the crack lies beneath the surface. Due to varying conditions in the interior of the specimen, the location of the crack tip is estimated by the following empirical equation

$$a_s = a_0 + 0.91 u_{20} \qquad (A.5)$$

where a_s is the estimated sharp crack tip length, a_0 is the surface blunted crack tip length, and u_{20} is the crack tip opening displacement (fig A2). The value of 0.91 was calculated by averaging several sets of data. By applying equation (A.3) at the new crack tip location, a_s, the displacement singularity can be obtained.

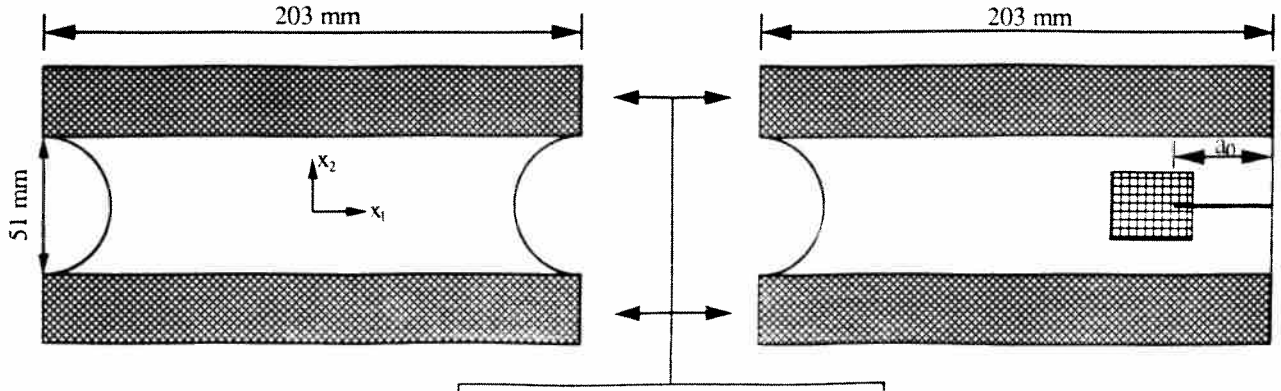

Figure 1
Uncracked biaxial specimen

Figure 2
Edge cracked biaxial specimen

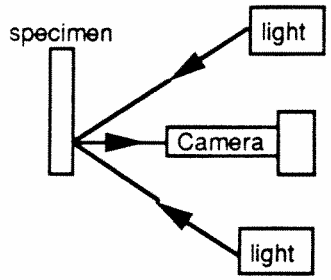

Figure 3. Camera Setup For Cracked Specimen

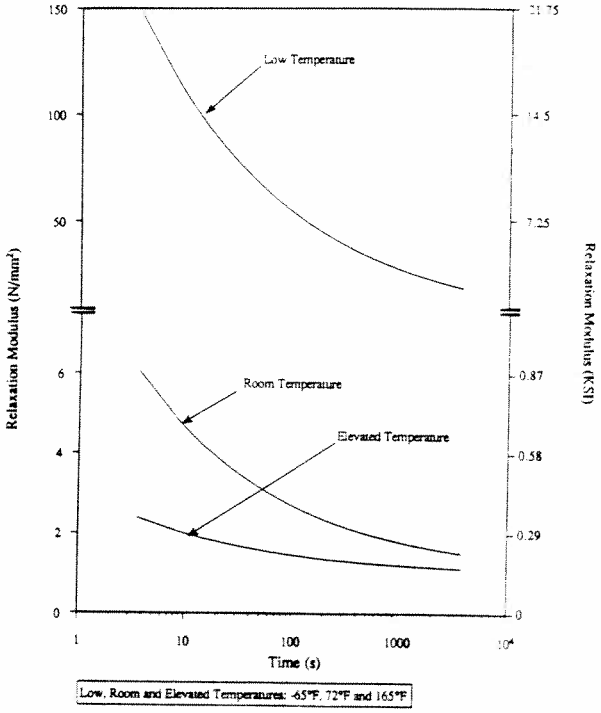

Figure 4 : Relaxation modulus verses time at -65, 72, 165 F

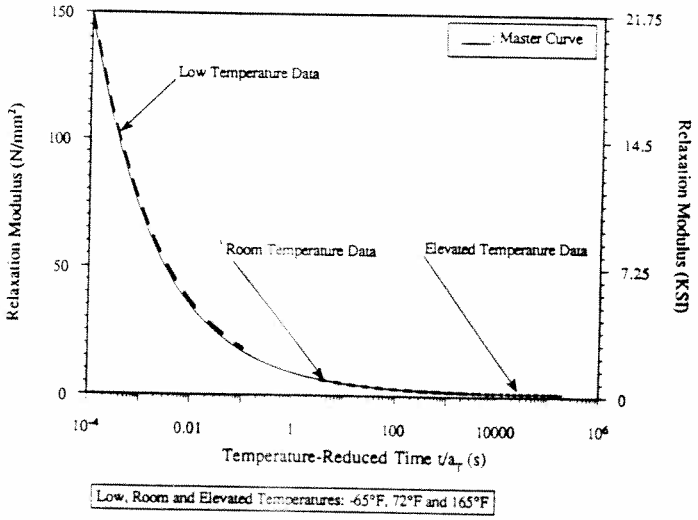

Figure 5 : Master curve of relaxation modulus at room temperature (72 F)

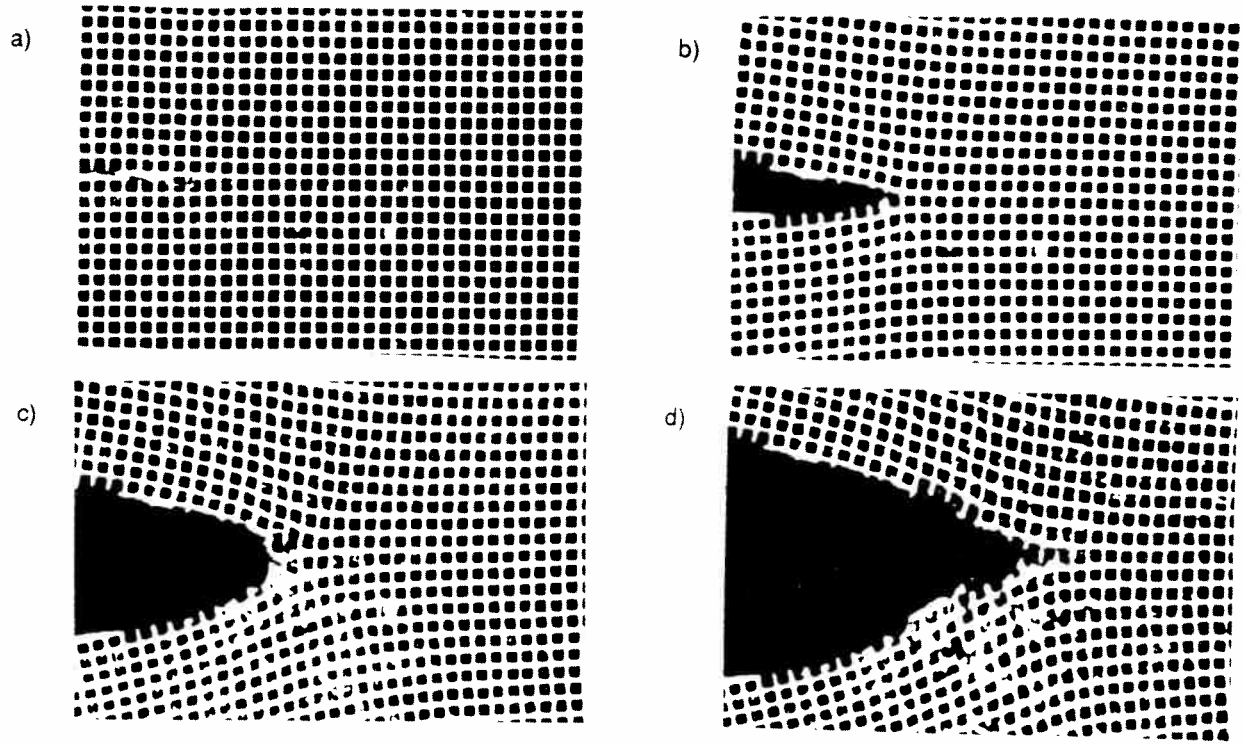

Figure 6: Stages of crack growth a) Undeformed b) Crack Opening
c) Crack Blunting d) Crack Propagation/Resharpening

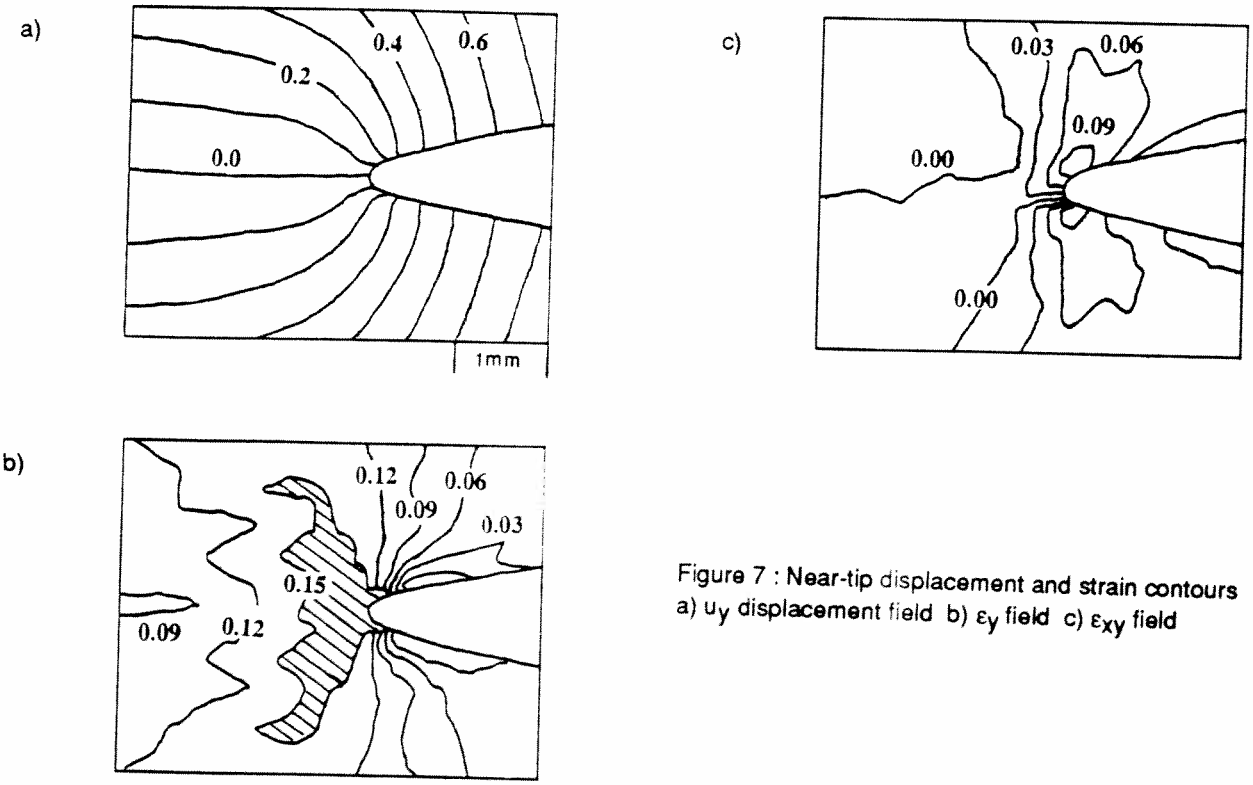

Figure 7 : Near-tip displacement and strain contours
a) u_y displacement field b) ε_y field c) ε_{xy} field

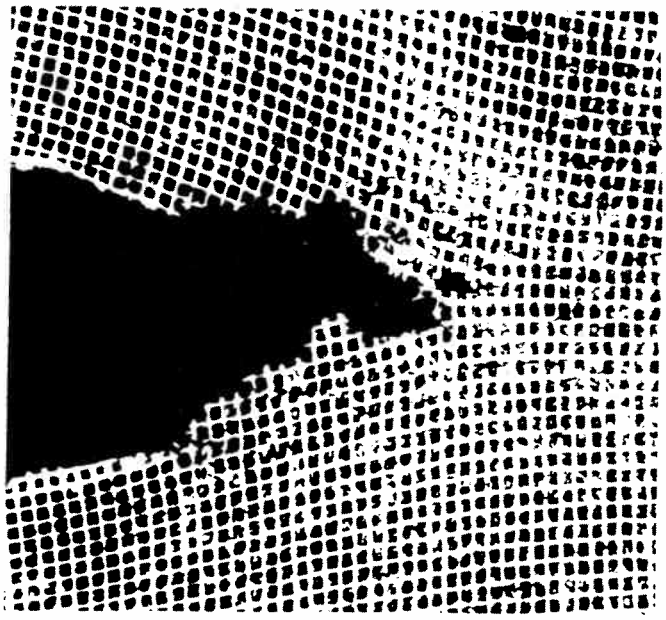

Figure 8 : Photograph displaying undulating path of crack growth

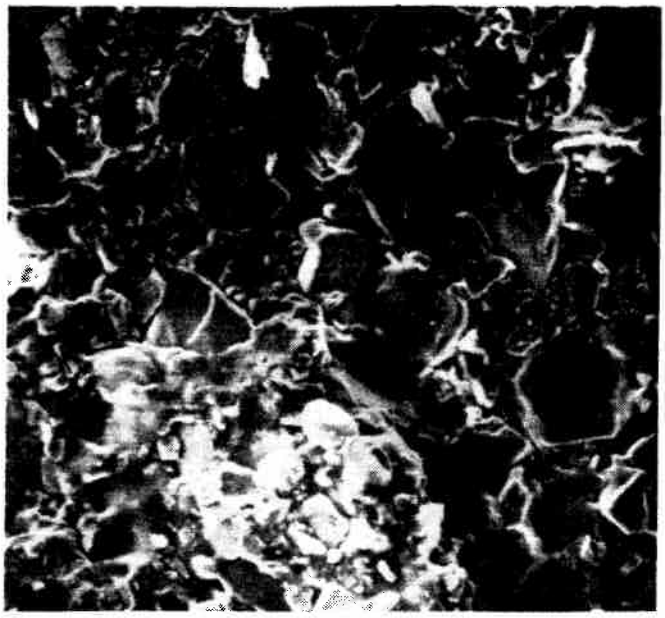

Figure 9 : 100 magnification SEM picture showing fracture surface

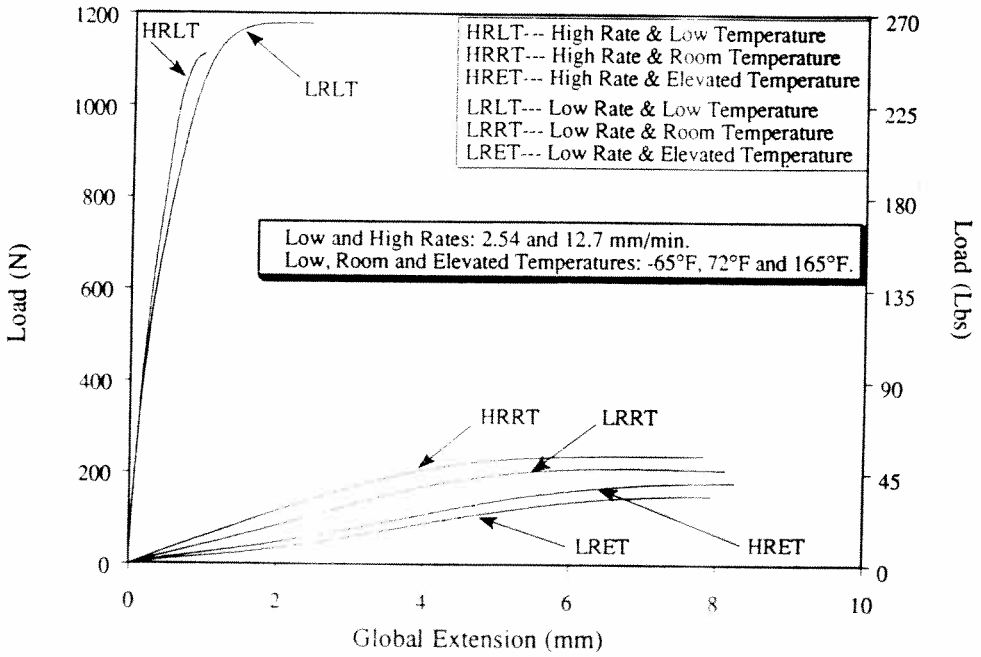

Figure 10 : Load variations for cracked thin specimen under three temperatures and two loading rates.

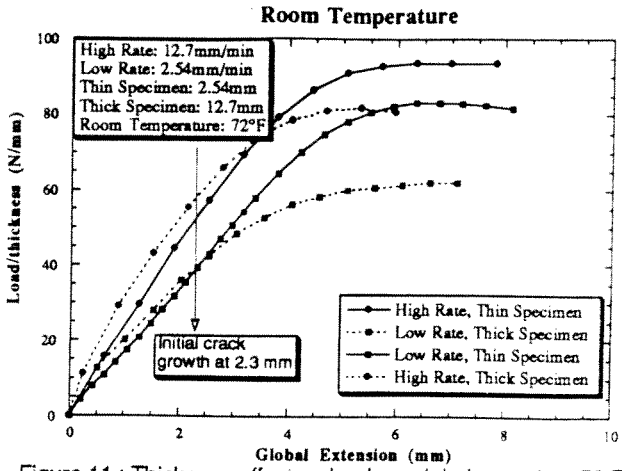

Figure 11 : Thickness effect on load vs. global extention, 72 F

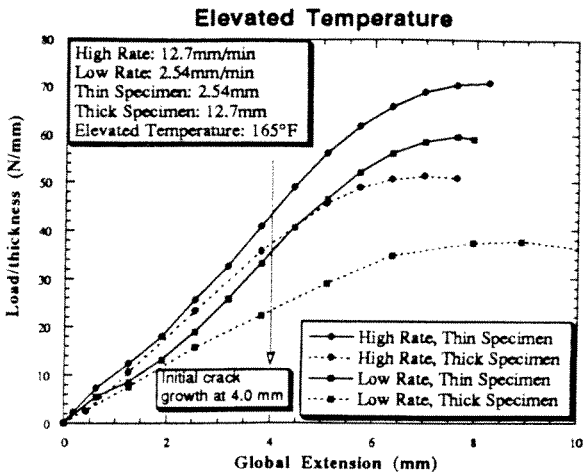

Figure 12 : Thickness effect on load vs. global extension, 165 F

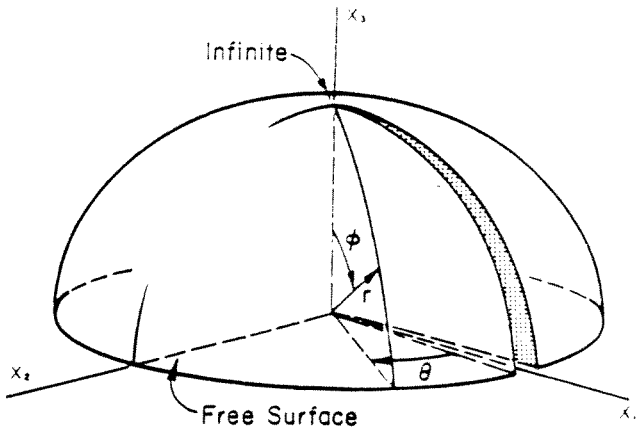

Figure A1 : Geometry used by Benthem to evaluate the displacement singularity

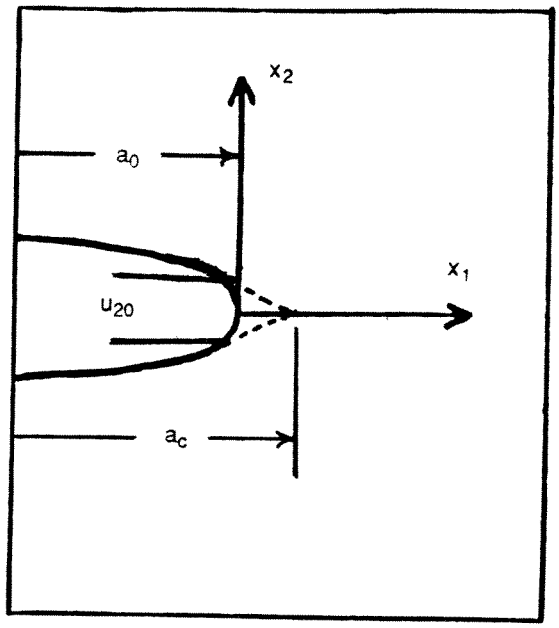

Figure A2 : Estimated sharp crack tip location for a blunt surface crack.